

NEOROCKS: COMPOSITIONAL PROPERTIES OF NEAR-EARTH OBJECTS FROM SKY SURVEYSA. V. Sergeev^{1,2}, B. Carry¹, and the NEOROCKS team*¹ Université Côte d'Azur, Observatoire de la Côte d'Azur, CNRS, Laboratoire Lagrange, France²V. N. Karazin Kharkiv National University, Kharkiv, 61022, Ukraine

* **Keywords:** *Minor planets, asteroids: NEOs - Techniques: photometric - Surveys*

Introduction: Asteroids are remnants of the building blocks that formed terrestrial planets and the cores of giant planets in the early Solar System 4.6 billion years ago. Among various dynamical classes of asteroids, near-Earth and Mars-crosser asteroids (NEAs and MCs) form a transient population with lifetimes of only a few million years before being ejected from the Solar System, falling into the Sun, or impacting a planet [1]. Near-Earth objects (NEOs), which include NEAs, MCs, and some Hungarias, are of both scientific and pragmatic interest. Their proximity to Earth enables better observation of smaller objects with ground-based telescopes and makes them favourable targets for space exploration due to the lower propulsion needed to reach them [2]. Furthermore, studying NEOs is essential for risk mitigation as they pose potential threats [3]. The NEOROCKS project [4] aims to characterize the population of near-Earth objects by studying the properties of a large corpus of NEOs.

Data sources: In this study, we collected and compared Near-Earth Object (NEO) color data from four recently published sources: Sloan Digital Sky Survey [5], SkyMapper Southern Survey [6], Gaia DR3 visible spectra [7, 8], and a compilation of ground-based spectra [9]. By converting the asteroid reflectance to colors, we aim to create a large, homogeneous dataset.

We gathered 11,142 individual multi-filter SDSS observations for 5,425 unique NEOs, remeasuring 470 NEO colors to address potential biases. The SkyMapper catalogue, with its various observing strategies, contains 12,001 individual observations for 3,149 unique NEOs. We retrieved 9,212

colors for 2,081 individual NEOs by limiting the observation time between filters to 20 minutes and weighting the mean color of multiple asteroid measurements. SkyMapper colors were converted to SDSS colors using color-transformation coefficients computed from a wide range of stellar classes [6].

The Gaia DR3 dataset contains 60,518 low-resolution reflectance spectra of asteroids, including 838 NEOs. While the ground-based spectra dataset contains 4,548 spectra of 3,157 unique asteroids among which we extracted 1,072 spectra for 846 unique NEOs and converted both reflectance datasets to SDSS colors to create a homogeneous dataset of NEO colors.

Before merging the four catalogs, we checked for systematic differences in colors and uncertainties among the datasets. We cross-matched asteroid colors from other sources to SDSS as a reference, finding shared asteroids and computing color differences. We then corrected the systematic biases for each color before merging the datasets for further analysis.

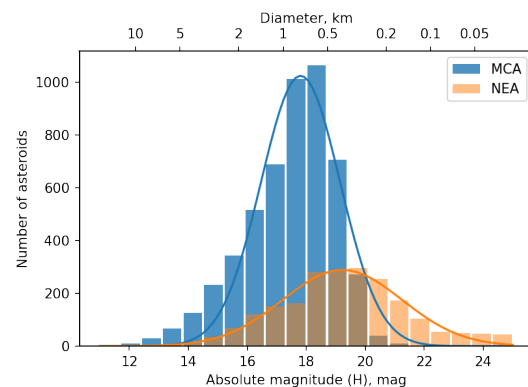


Figure 1: Distribution of absolute magnitude of Mars-crossers (blue) and Near-Earth (orange) asteroids . The diameter scale is a guideline, computed with an average albedo of 0.24.

The most numerous fraction of merged datasets belonging to the SDSS sample contains 4,398 unique NEOs, followed by SkyMapper 964, ground-based 507, and Gaia 199. For NEOs present in more than one catalog, we select the color with the smallest uncertainty. With these results we built the NEOs NEOROCKS catalog,

*The NEOROCKS team: M. Marsset, P. Pravec, D. Perna, F. E. DeMeo, V. Petropoulou, M. Lazzarin, F. La Forgia, I. Di Petro, E. Dotto, M. Banaszekiewicz, S. Banchi, M.A. Barucci, F. Bernardi, M. Birlan, A. Cellino, J. De Leon, M. Lazzarin, E. Mazzotta Epifani, A. Medavilla, J. Nomen Torres, E. Perozzi, C. Snodgrass, C. Teodorescu, S. Anghel, A. Bertolucci, F. Calderini, F. Colas, A. Del Vigna, A. Dell'Oro, A. Di Cecco, L. Dimare, P. Fatka, S. Fornasier, E. Frattin, P. Frosini, M. Fulchignoni, R. Gabryszewski, M. Giardino, A. Giunta, T. Hromakina, J. Huntingford, S. Ieva, J.P. Kotlarz, M. Popescu, J. Licandro, H. Medeiros, F. Merlin, F. Pinna, G. Polenta, A. Rozek, P. Scheirich, A. Sonka, G.B. Valsecchi, P. Wajer, A. Zinzi.

comprising 7,401 NEOs with at least one color measurement.

The orbital distribution of the NEOROCKS sample includes 2,277 NEOs and 5,124 Mars-Crossers. The absolute magnitudes in the NEOs NEOROCKS catalog exhibit a bimodal distribution, reflecting the typical larger distance of Mars-Crossers compared with Near-Earth Asteroids (NEAs). We assume an albedo of 0.24 for all NEOs, resulting in average diameters of 400m for NEAs and 760m for Mars-Crossers, covering a range from approximately 10 km down to 50 m (see Figure 1).

Taxonomy: Taxonomy is vital for categorizing Near-Earth Objects (NEOs) based on their shared properties, helping to better understand and mitigate potential threats. Asteroid taxonomy relies on the similarity of spectral signatures of light reflected by their surfaces to spectral templates [10, 11].

The taxonomic classification of NEOs is important due to the growing number of discoveries, and while spectroscopy is accurate, it requires time-consuming observations. Photometry data, in contrast, is more efficient and practical for large-scale surveys [12, 13, 14].

We used an approach adapted for multi-color photometry [15, 16, 5], based on the recent taxonomy of M. Mahlke [9], an update of the widely used scheme of Bus-DeMeo taxonomy [17]. The updated taxonomy and a probabilistic method were used to compute probabilities for each asteroid to belong to one of ten broad taxonomic complexes.

We also build a single-color classification based on the g-r color, allowing discrimination between "red" and "blue" objects [18]. Although cruder, the single-color classification has merit. The two classification methods, one using three colors (g-r, g-i, i-z) and the other using a single color (g-r), are merged, with the former preferred over the latter.

The distribution of taxonomy and albedos reveals the prevalence of silicate asteroid types in the NEO population, though this result could be distorted by observation bias. The NEO dataset was compared with previous surveys such as MITHNEOS, NEOSHIELD, and MANOS (Binzel et al., 2019; Perna et al., 2018; Devogèle et al., 2019), with an overall good agreement between these datasets.

Future space mission targets:

The Solar System, in contrast to other astrophysical domains, is relatively close, enabling

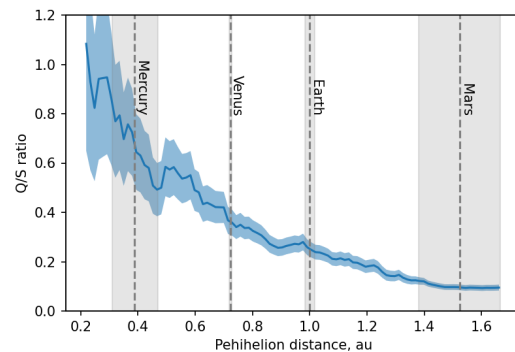


Figure 2: Running mean of the ratio between the number of Q and S asteroids as function of perihelion.

space missions to make significant discoveries. Since the 1990s, studies have been conducted to find asteroid flyby candidates during interplanetary missions [19, 20].

The NEOROCKS NEOs data was employed to analyze the composition of potential candidates for upcoming space missions [21, 22], which included approximately one hundred candidates for the ESA Hera mission [23]. A critical parameter for target selection is the energy required, expressed as Δv . Our data contains the taxonomy of 42 mission-accessible NEOs with a $\Delta v < 6.5$ km. We also found Gaia spectra for two candidates out of the short list of seven candidates still consider for a flyby by Hera mission.

Discussion: We used the NEOs NEOROCKS catalog to study space weathering. Our sample contains 1,175 weathered S-type and 196 fresh Q-type silicate asteroids. We found, that the spectral slope of S-type asteroids is constant for asteroids smaller than about 1-5 km, and increases for larger asteroids. We also found that the Q/S ratio is increasing toward to small diameter, but falls for the smallest NEOs, which may be attributed to the increasing number of monoliths, for which resurfacing may be difficult. Our analysis shows a clear trend of increasing spectral slope of S-types with a more distant perihelion till about 0.8 au. There is also a strong correlation between the Q/S ratio and the perihelion distance, with the fraction of Q types increasing across a wide range of distances from 0.2 to 1.6 au (see Figure 2). We did not find a correlation between space weathering and minimum orbit insertion distance (MOID) as well as the inclination of asteroid orbits.

We also explored the distribution of A-type asteroids, which are rare in the main belt and exhibit an olivine-rich composition. We report a significantly higher fraction of A-types ($2.5 \pm 0.2\%$) among NEOs than in the main belt (0.16%), as reported by DeMeo et al., 2019. A-types are mainly concentrated between the orbit of Mars and the 4:1 resonance with Jupiter, with most NEOs related to the Hungarians. In this region, the fraction of A-type asteroids increases to 4%. That indicates that certain A-type asteroids could be fragments that were ejected from Mars.

We finally employed the seven-regions source model of Granvik et al. (2018) to predict the taxonomy of small asteroids in these regions, using the taxonomy of the NEOROCKS NEO sample. The most abundant source of NEOs is the ν_6 region, which limits the inner border of the main belt. We predict it to be dominated by mafic-silicate-rich asteroids. The distribution of taxonomic classes is almost similar for the other source regions in the inner belt: the 3:1 MMR limiting the inner and middle belt, and the Phocaea and Hungaria regions. The fraction of mafic-silicate-rich asteroids decreases for source regions located further from the Sun (5:2 and 2:1 MMR, JFC) in that is dominated by opaque-rich asteroids (B, C, D).

Conclusion: We analyzed a comprehensive sample of planet-crossing asteroids, integrating broad-band photometry from SDSS and SMSS surveys, along with reflectance spectroscopy from ESA Gaia mission and ground-based observations. We determine the taxonomy of 7,401 NEOs, ranging from 10 km to 50 m in diameter. The sample predominantly consists of S-type asteroids (about 45%), similar to other NEO surveys. However, the proportion of S-types may be overestimated due to observational bias. Additionally, we find a significantly higher fraction (up to 4%) of A-type asteroids among NEOs compared to the Main Belt. These A-types concentrate in semi-major axis ranges between 1.5 and 2 au. We confirm a strong dependence of the spectral slope of S-types on perihelion using a sample of over a thousand objects. The slope distribution aligns with the rejuvenation model through thermal fatigue proposed recently [24].

References: [1] B. J. Gladman, et al. (1997) *Science* 277:197 doi. [2] P. Abell, et al. (2012) in *AAS/Division for Planetary Sciences Meeting Abstracts* vol. 44. [3] L. Drube, et al. (2015) in *Handbook of Cosmic Hazards and Planetary Defense* 763–790 doi. [4] E. Dotto, et al. (2021) in *7th IAA Planetary Defense*

Conference 221. [5] A. V. Sergeev, et al. (2021) *A&A* 652:A59 doi.arXiv:2108.05749. [6] A. V. Sergeev, et al. (2022) *A&A* 658:A109 doi.arXiv:2110.11656. [7] G. Collaboration, et al. (2016) *A&A* 595:A1 doi. [8] L. Galluccio, et al. (2022) *arXiv e-prints* arXiv:2206.12174.arXiv:2206.12174. [9] M. Mahlke, et al. (2022) *A&A* 665:A26 doi.arXiv:2203.11229. [10] I. Belskaya, et al. (2015) in *Asteroids IV* 151–163 doi. [11] V. Reddy, et al. (2015) in *Asteroids IV* 43–63 doi. [12] D. Nesvorný, et al. (2005) *Icarus* 173:132 doi. [13] A. Parker, et al. (2008) *Icarus* 198:138 doi. [14] B. Carry, et al. (2016) *Icarus* 268:340 doi. [15] F. E. DeMeo, et al. (2013) *Icarus* 226(1):723 doi. arXiv:1307.2424. [16] M. Popescu, et al. (2018) *A&A* 617:A12 doi.arXiv:1807.00713. [17] F. DeMeo, et al. (2009) *Icarus* 202:160 doi. [18] N. Erasmus, et al. (2020) *ApJS* 247(1):13 doi. arXiv:2002.08135. [19] M. Di Martino, et al. (1990) *Icarus* 87(2):372 doi. [20] L. Agostini, et al. (2022) *Planet. Space Sci.* 216:105476 doi. [21] D. J. Scheeres, et al. (2020) in *51st Annual Lunar and Planetary Science Conference Lunar and Planetary Science Conference 1965*. [22] H. Yano, et al. (2022) in *44th COSPAR Scientific Assembly. Held 16-24 July* vol. 44 3264. [23] A. Fitzsimmons, et al. (2020) in *European Planetary Science Congress EPSC2020–1064*. [24] K. J. Graves, et al. (2019) *Icarus* 322:1 doi.